

Toward full result for NLO dijet production in proton-nucleus collisions

Yair Mulian
Jyvaskyla University

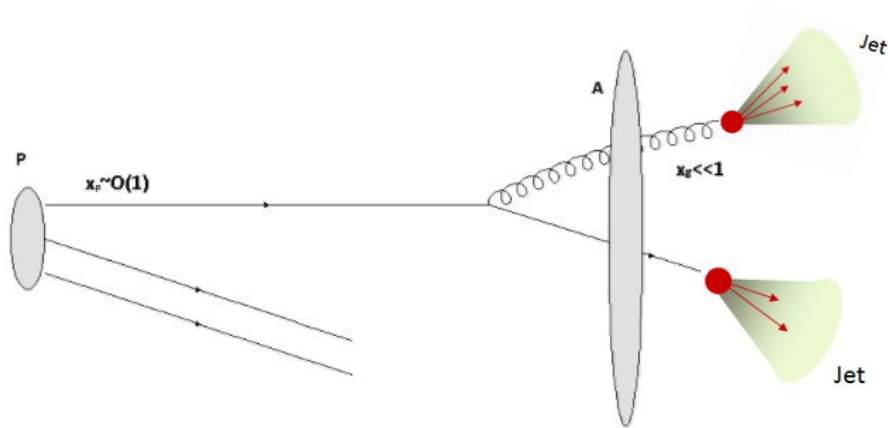
Based on hep-ph/1809.05526,
hep-ph/2009.11930 (with E. Iancu)



Forward Jet Production

The basic setup: a large- x parton from the proton scatters off the small- x gluon distribution in the target nucleus. The large- x parton is most likely a quark. We adopt the formalism of the LC outgoing state, using the CGC effective theory together with the hybrid factorization.

The LO result appears in hep-ph/0708.0231 (C. Marquet).



Quark fragmentation in the presence of a shockwave.

The Outgoing State Formalism

The time evolution of the initial (bare) quark state is given by:

$$|q_\lambda^\alpha(q^+, \mathbf{q})\rangle_{\text{in}} \equiv U(0, -\infty) |q_\lambda^\alpha(q^+, \mathbf{q})\rangle$$

Where U denotes the unitary operator, defined as

$$U(t, t_0) = \text{T exp} \left\{ -i \int_{t_0}^t dt_1 H_I(t_1) \right\}$$

The quark outgoing state is given by:

$$|q_\lambda^\alpha(q^+, \mathbf{w})\rangle_{\text{out}} \equiv U(\infty, 0) \hat{S} U(0, -\infty) |q_\lambda^\alpha(q^+, \mathbf{w})\rangle$$

This state encodes the information both on the **time evolution** and **interaction with the target nucleus** of the incoming quark state.

The expectation values of operators are directly related to the outgoing state:

$$\langle \hat{O} \rangle = \left\langle {}_{\text{out}} \langle q_\lambda^\alpha(q^+, \mathbf{w}) | \hat{O} | q_\lambda^\alpha(q^+, \mathbf{w}) \rangle_{\text{out}} \right\rangle_{\text{egc}}$$

The LO Outgoing State

The outgoing state at leading order is given by

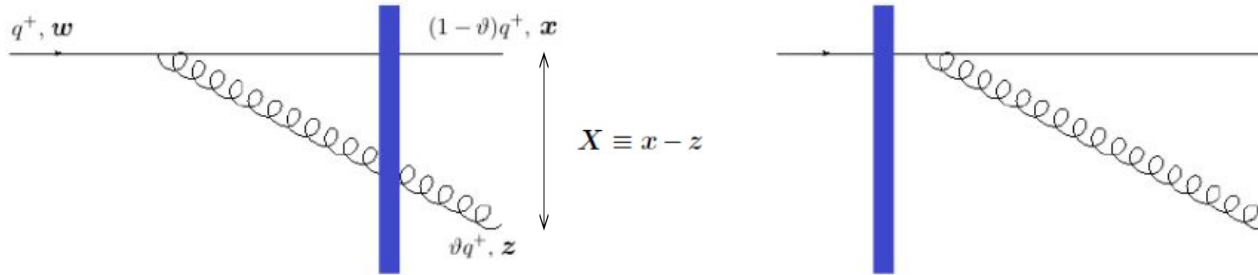
$$|q_\lambda^\alpha(q^+, \mathbf{w})\rangle_{out} \equiv U(\infty, 0) \hat{S} U(0, -\infty) |q_\lambda^\alpha(q^+, \mathbf{w})\rangle = \mathbf{z} |q_\lambda^\alpha(q^+, \mathbf{w})\rangle + |\psi_\lambda^\alpha(q^+, \mathbf{w})\rangle_{qg}$$

The additional term reads:

$$|\psi_\lambda^\alpha(q^+, \mathbf{w})\rangle_{qg} = \int_{\mathbf{x}, \mathbf{z}} \int_0^1 d\vartheta \frac{ig\sqrt{q^+}}{4\pi^{3/2}} \frac{\phi_{\lambda_1\lambda}^{ij}(\vartheta)}{\sqrt{\vartheta}} \frac{\mathbf{X}^j}{\mathbf{X}^2} \delta^{(2)}(\mathbf{w} - (1-\vartheta)\mathbf{x} - \vartheta\mathbf{z})$$

$$\times \left[V^{\gamma\beta}(\mathbf{x}) U^{ba}(\mathbf{z}) t_{\beta\alpha}^a - t_{\gamma\beta}^b V^{\beta\alpha}(\mathbf{w}) \right] \left| q_{\lambda_1}^\gamma((1-\vartheta)q^+, \mathbf{x}) g_i^b(\vartheta q^+, \mathbf{z}) \right\rangle$$

Diagrammatically:



$$\vartheta \equiv k^+/q^+$$

$$U(x) = \text{T exp} \left\{ ig \int dx^+ T^a A_a^-(x^+, \mathbf{x}) \right\}$$

$$V(x) = \text{T exp} \left\{ ig \int dx^+ t^a A_a^-(x^+, \mathbf{x}) \right\}$$

Blue bar denotes a shockwave = interaction with the target.

The LO Forward Dijet Cross Section

From the production state we can pass easily to the quark-gluon dijet cross section:

$$\frac{d\sigma_{\text{LO}}^{qA \rightarrow qg+X}}{d^3k d^3p} \equiv \frac{1}{2N_c L} \text{out} \langle q_\lambda^\alpha(q^+, \mathbf{q}) | \hat{N}_q(p) \hat{N}_g(k) | q_\lambda^\alpha(q^+, \mathbf{q}) \rangle_{\text{out}}$$

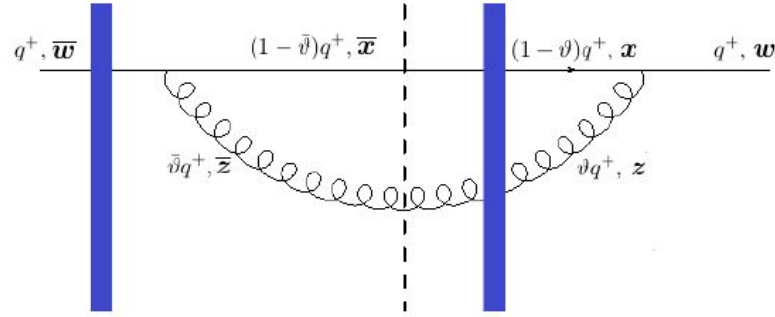
The following number density operators were introduced:

$$\hat{N}_q(p) \equiv \frac{1}{(2\pi)^3} b_\lambda^{\alpha\dagger}(p) b_\lambda^\alpha(p) \quad \hat{N}_g(k) \equiv \frac{1}{(2\pi)^3} a_i^{a\dagger}(k) a_i^a(k)$$

Then the result for the leading-order dijet cross section is given by (at large N_c):

$$\begin{aligned} \frac{d\sigma_{\text{LO}}^{qA \rightarrow qg+X}}{dk^+ d^2\mathbf{k} dp^+ d^2\mathbf{p}} &= \frac{2\alpha_s C_F}{(2\pi)^6 q^+} \frac{(1 + (1 - \vartheta)^2)}{\vartheta} \delta(q^+ - k^+ - p^+) \\ &\times \int_{\mathbf{x}, \bar{\mathbf{x}}, \mathbf{z}, \bar{\mathbf{z}}} \frac{\mathbf{X} \cdot \bar{\mathbf{X}}}{\mathbf{X}^2 \bar{\mathbf{X}}^2} e^{-i\mathbf{p} \cdot (\mathbf{x} - \bar{\mathbf{x}}) - i\mathbf{k} \cdot (\mathbf{z} - \bar{\mathbf{z}})} \\ &\times [Q(\mathbf{x}, \mathbf{z}, \bar{\mathbf{z}}, \bar{\mathbf{x}}) \mathcal{S}(\mathbf{z}, \bar{\mathbf{z}}) - \mathcal{S}(\mathbf{x}, \mathbf{z}) \mathcal{S}(\mathbf{z}, \bar{\mathbf{w}}) - \mathcal{S}(\mathbf{w}, \bar{\mathbf{z}}) \mathcal{S}(\bar{\mathbf{z}}, \bar{\mathbf{x}}) + \mathcal{S}(\mathbf{w}, \bar{\mathbf{w}})] \end{aligned}$$

An example for contribution which is included in the result, $\mathcal{S}(\mathbf{x}, \mathbf{z}) \mathcal{S}(\mathbf{z}, \bar{\mathbf{w}})$:



The dashed line, “the cut”, is the final state (the detector). The dipole and quadropole are defined by:

$$\mathcal{S}(\bar{\mathbf{w}}, \mathbf{w}) \equiv \frac{1}{N_c} \text{tr} \left[V^\dagger(\bar{\mathbf{w}}) V(\mathbf{w}) \right] \quad \mathcal{Q}(\bar{\mathbf{x}}, \mathbf{x}, \mathbf{z}, \bar{\mathbf{z}}) \equiv \frac{1}{N_c} \text{tr} \left[V^\dagger(\bar{\mathbf{x}}) V(\mathbf{x}) V^\dagger(\mathbf{z}) V(\bar{\mathbf{z}}) \right]$$

From the partonic cross section we can find the quark channel contribution by convolution with the PDF:

$$\left. \frac{d\sigma_{\text{LO}}^{pA \rightarrow 2jet+X}}{d^3p d^3k} \right|_{q\text{-channel}} = \int dx_p q_f(x_p, \mu^2) \frac{d\sigma_{\text{LO}}^{qA \rightarrow qg+X}}{d^3p d^3k}$$

For measuring two hadrons one has to convolute the result above with the fragmentation functions:

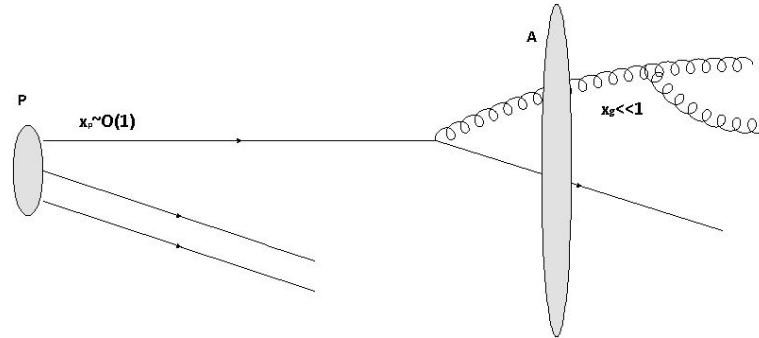
$$\left. \frac{d\sigma_{\text{LO}}^{pA \rightarrow h_1 h_2 + X}}{d^3p d^3k} \right|_{q\text{-channel}} = \int \frac{dz_1}{z_1^3} \int \frac{dz_2}{z_2^3} \int dx_q q_f(x_q, \mu^2) \frac{d\sigma_{\text{LO}}^{qA \rightarrow qg+X}}{d^3p_1 d^3k_1} D_{h_1/q}(z_1, \mu^2) D_{h_2/g}(z_2, \mu^2)$$

The Trijet Setup

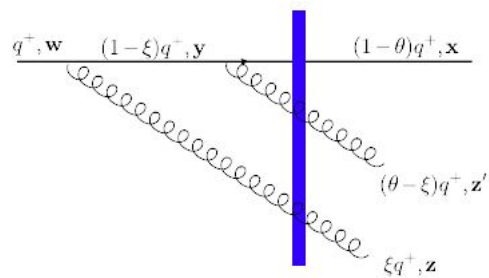
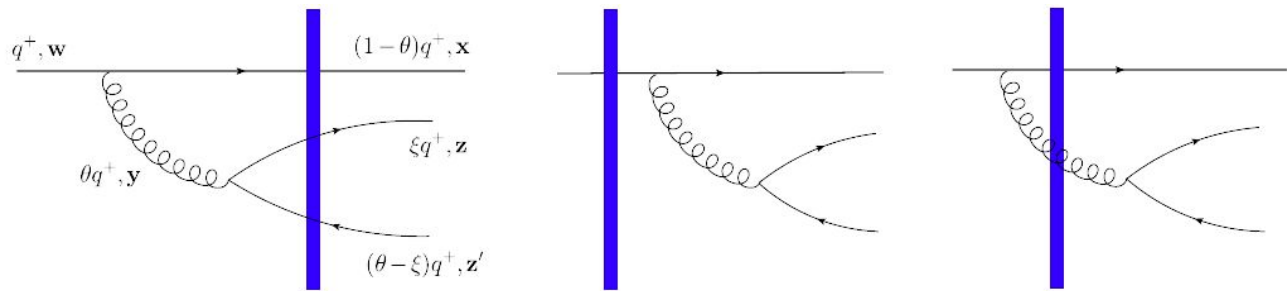
Two possible configurations of 3 particles in the final state:

- a) **Quark, quark and anti-quark,**
- b) **Quark together with two gluons.**

The production of these configurations happen via two successive parton splittings (in the light-cone formalism, there are also 1- \rightarrow 3 instantaneous vertices).



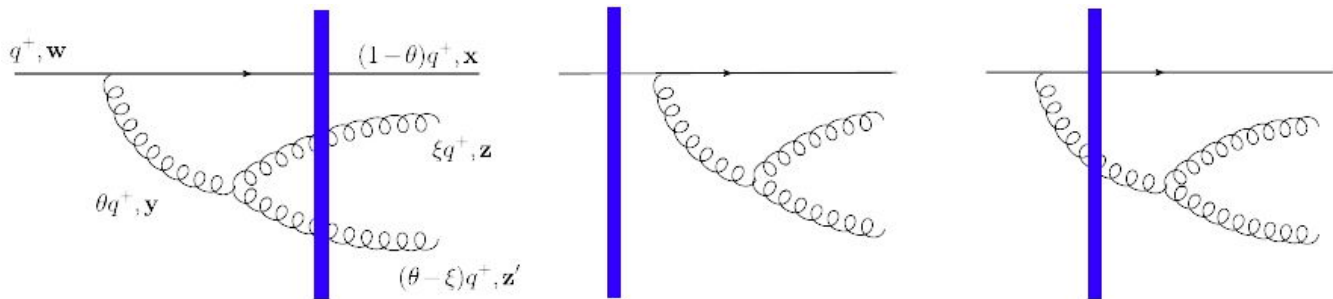
An example for a contribution with 3 particles in the final state



(a)

(b)

(c)



From Trijet to “real” NLO Dijet

The two contributions to the cross section are:

$$\frac{d\sigma^{qA \rightarrow qq\bar{q}+X}}{d^3q_1 d^3q_2 d^3q_3} \equiv \frac{1}{2N_c L} \text{out} \langle q_\lambda^\alpha(q^+, \mathbf{q}) | \hat{\mathcal{N}}_q(q_1) \hat{\mathcal{N}}_q(q_2) \hat{\mathcal{N}}_{\bar{q}}(q_3) | q_\lambda^\alpha(q^+, \mathbf{q}) \rangle_{\text{out}}$$

$$\frac{d\sigma^{qA \rightarrow qgg+X}}{d^3q_1 d^3q_2 d^3q_3} \equiv \frac{1}{2N_c L} \text{out} \langle q_\lambda^\alpha(q^+, \mathbf{q}) | \hat{\mathcal{N}}_q(q_1) \hat{\mathcal{N}}_g(q_2) \hat{\mathcal{N}}_g(q_3) | q_\lambda^\alpha(q^+, \mathbf{q}) \rangle_{\text{out}}$$

The trijet cross section is given by their sum:

$$\frac{d\sigma^{pA \rightarrow 3jet+X}}{d^3q_1 d^3q_2 d^3q_3} = \int dx_p q(x_p, \mu^2) \left(\frac{d\sigma^{qA \rightarrow qgg+X}}{d^3q_1 d^3q_2 d^3q_3} + \frac{d\sigma^{qA \rightarrow qq\bar{q}+X}}{d^3q_1 d^3q_2 d^3q_3} \right)$$

The real dijet cross section is related to trijet cross section by the integration over the unmeasured parton:

$$\frac{d\sigma_R^{qA \rightarrow 2jet+X}}{d^3q_1 d^3q_2} = \int d^3q_3 \frac{d\sigma^{qA \rightarrow 3jet+X}}{d^3q_1 d^3q_2 d^3q_3}$$

The Trijet Cross Section

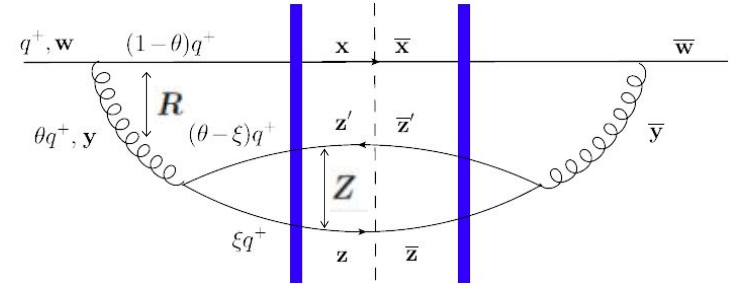
The quark quark anti-quark contribution reads:

$$\frac{d\sigma^{qA \rightarrow qq\bar{q}+X}}{dk_1^+ d^2k_1 dk_2^+ d^2k_2 dk_3^+ d^2k_3} = \frac{\alpha_s^2 C_F N_f}{2(2\pi)^{10} (q^+)^2} \delta(q^+ - k_1^+ - k_2^+ - k_3^+)$$

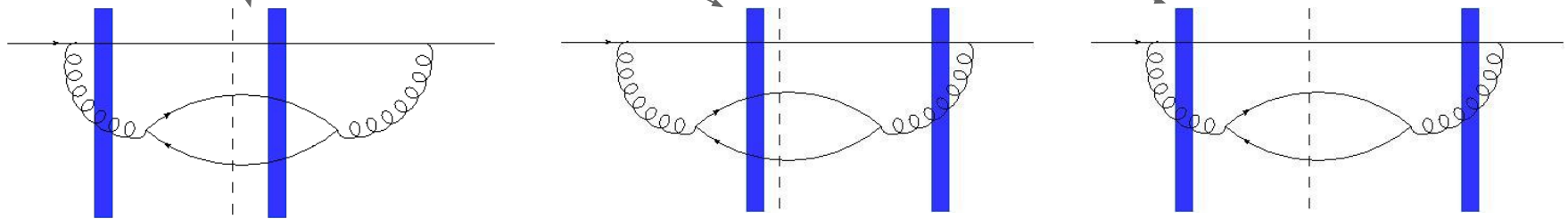
$$\times \int_{\bar{x}, \bar{z}, \bar{z}', x, z, z'} e^{-ik_1 \cdot (x - \bar{x}) - ik_2 \cdot (z - \bar{z}) - ik_3 \cdot (z' - \bar{z}')} \frac{R^i Z^j \bar{R}^m \bar{Z}^n}{Z^2 \bar{Z}^2}$$

$$\times \left[\mathcal{K}_0^{ijmn}(x, z, z', \bar{x}, \bar{z}, \bar{z}', \vartheta, \xi) \mathcal{W}_0(x, z, z', \bar{x}, \bar{z}, \bar{z}') \right]$$

$$\left[-(z, z' \rightarrow y) - (\bar{z}, \bar{z}' \rightarrow \bar{y}) + (z, z' \rightarrow y \ \& \ \bar{z}, \bar{z}' \rightarrow \bar{y}) \right] + (k_1^+ \leftrightarrow k_2^+, k_1 \leftrightarrow k_2).$$



$$y \equiv \frac{\xi z + (\vartheta - \xi) z'}{\vartheta}$$



The kernel:

$$\mathcal{K}_0^{ijmn}(x, z, z', \bar{x}, \bar{z}, \bar{z}', \vartheta, \xi) \equiv \frac{\Phi_{\lambda_3\lambda_2\lambda_1\lambda}^{ij}(x, z, z', \vartheta, \xi) \Phi_{\lambda_3\lambda_2\lambda_1\lambda}^{mn*}(\bar{x}, \bar{z}, \bar{z}', \vartheta, \xi)}{[\vartheta^2(1-\vartheta)\mathbf{R}^2 + \xi(\vartheta-\xi)\mathbf{Z}^2] [\vartheta^2(1-\vartheta)\bar{\mathbf{R}}^2 + \xi(\vartheta-\xi)\bar{\mathbf{Z}}^2]}$$

The effective vertex contain the information about both the reg. and inst. Interactions.

$$\Phi_{\lambda_3\lambda_2\lambda_1\lambda}^{jl}(x, z, z', \vartheta, \xi) \equiv \vartheta(1-\vartheta)\varphi_{\lambda_2\lambda_3}^{il}\left(\frac{\xi}{\vartheta}\right) \phi_{\lambda_1\lambda}^{ij}(\vartheta) - \delta_{\lambda_2\lambda_3}\delta_{\lambda_1\lambda}\delta^{jl} \frac{2(1-\vartheta)\xi(\vartheta-\xi)}{\vartheta} \frac{\mathbf{Z}^2}{\mathbf{R}\cdot\bar{\mathbf{Z}}}$$

For the color structure (at large N_c):

$$W_0(x, z, z', \bar{x}, \bar{z}, \bar{z}') \simeq Q(x, z', \bar{z}', \bar{x}) S(z, \bar{z}) - S(z, \bar{w}) S(x, z') - S(w, \bar{z}) S(\bar{z}', \bar{x}) + S(w, \bar{w})$$

And the longitudinal momentum fractions:

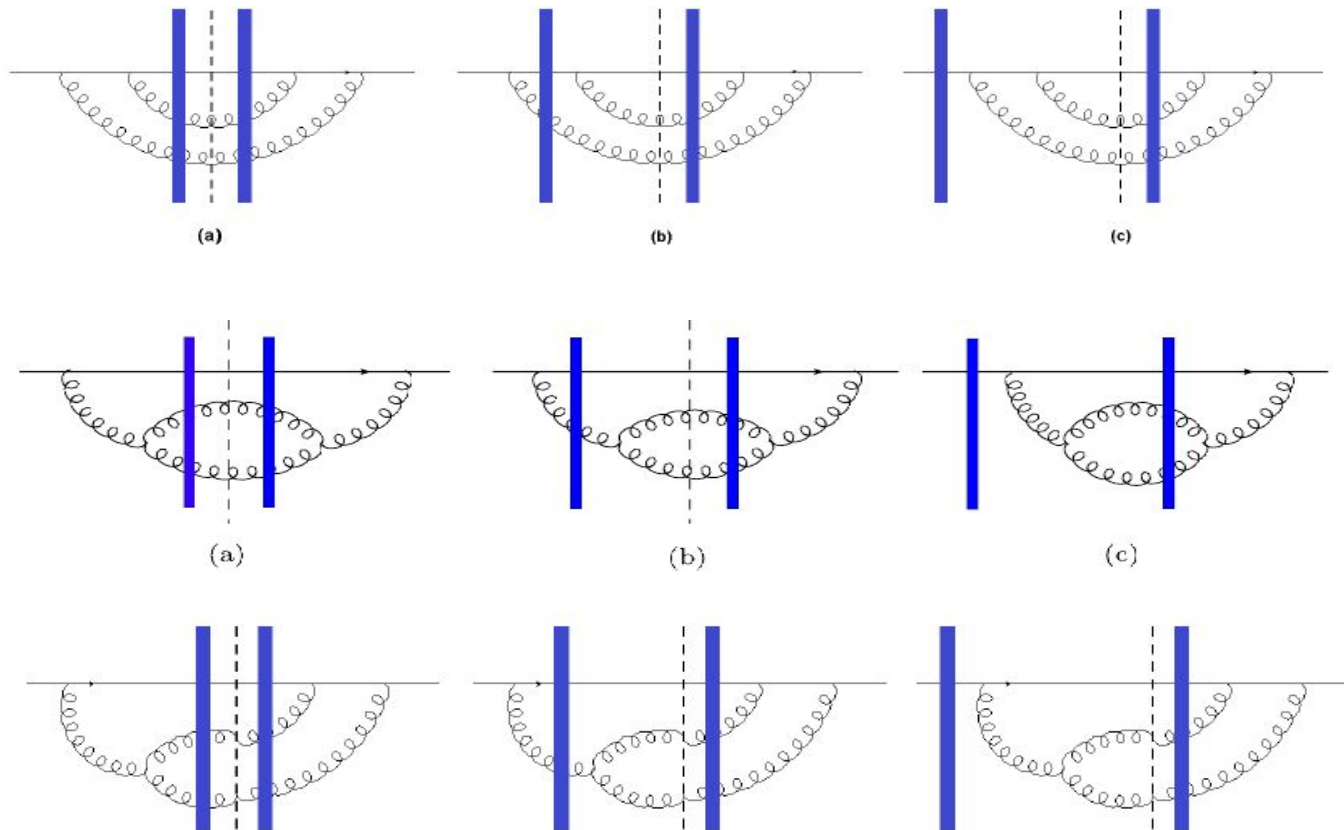
$$\vartheta = 1 - \frac{k_1^+}{q^+} \quad \xi = \frac{k_2^+}{q^+}$$

The replacement $(z, z' \rightarrow y)$ affects both the energy denominator and the Wilson lines:

$$\frac{1}{\vartheta^2(1-\vartheta)\mathbf{R}^2 + \xi(\vartheta-\xi)\mathbf{Z}^2} \longrightarrow \frac{1}{\vartheta^2(1-\vartheta)\mathbf{R}^2}$$

$$\left[V(\mathbf{y}) t^a V^\dagger(\mathbf{y}) \right]_{\alpha\beta} \longrightarrow t_{\alpha\beta}^b U^{ba}(\mathbf{y})$$

Gluons Contributions to Trijet Production



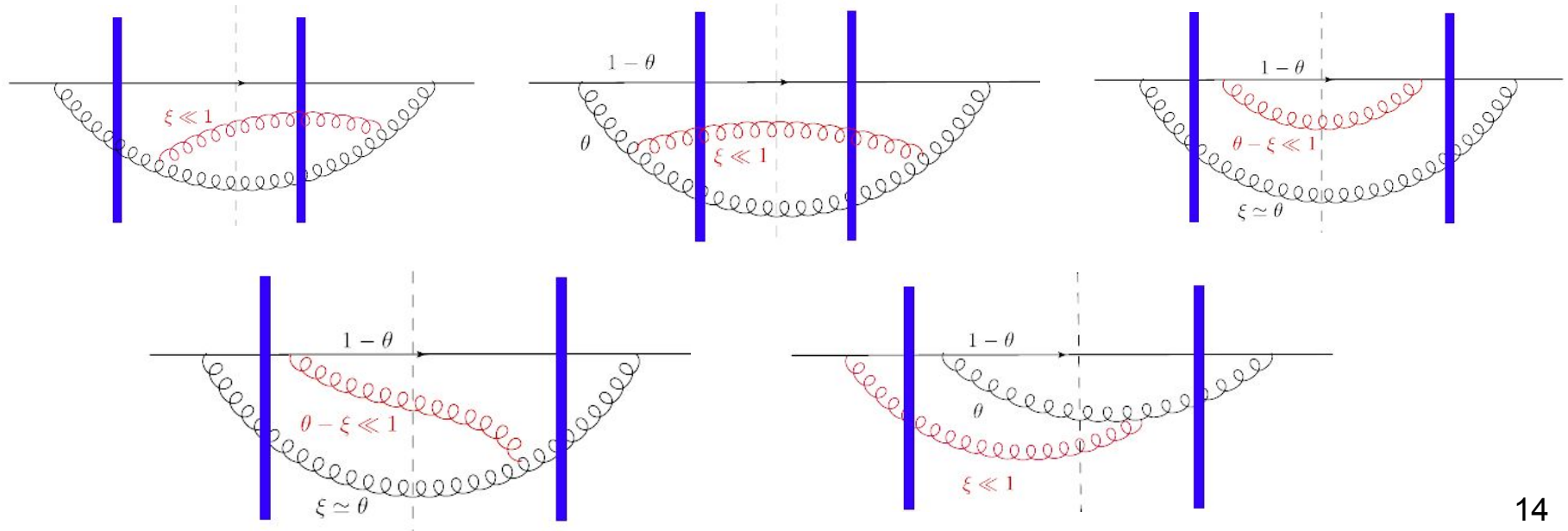
The QCD Divergences

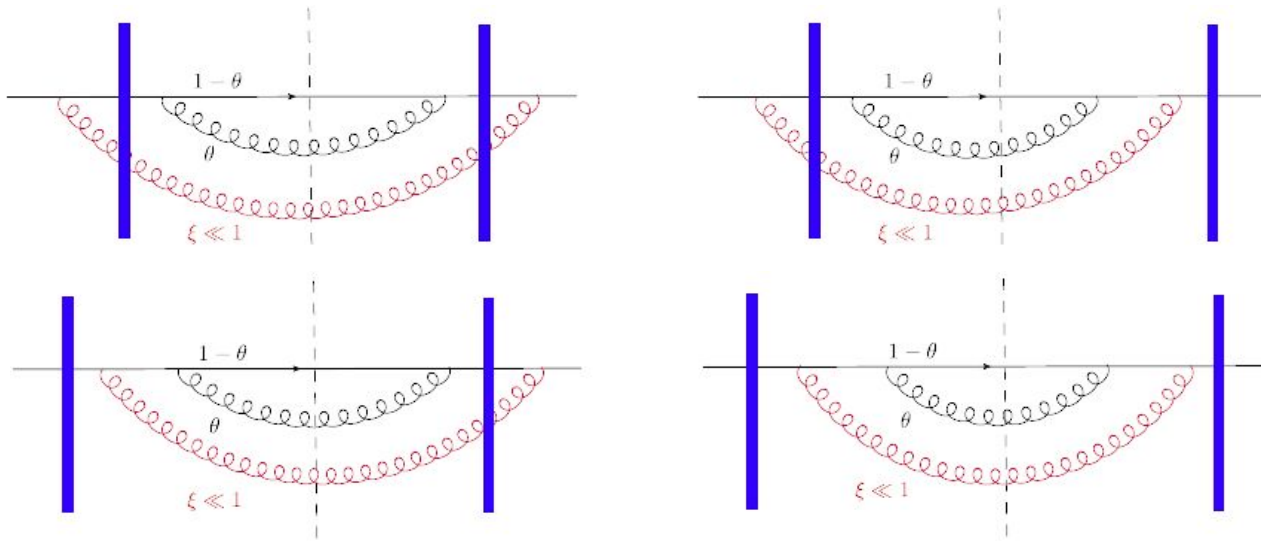
The divergences which are involved in the computation of QCD cross sections:

- 1) **Short distance poles**: when the partons are approaching each other (manifestly canceled by pairing diagrams).
- 2) **Collinear**: when partons are emitted far away from each other. Reabsorbed in DGLAP for the incoming PDF and outgoing fragmentation functions.
- 3) **UV divergences**: contribution to the beta function (regularized by dimreg).
- 4) **Soft**: these will occur when the longitudinal momentum of a gluon is vanishing. Canceled when summing the relevant contributions.

Recovering the B-JIMWLK Evolution

In the limit when one of the gluons become soft (eikonal emission vertex = no recoil of the emitter), the general NLO result has to reduce to one step in the real part of B-JIMWLK evolution of the leading order dijet production result. We managed to show that this is indeed the case in our result.



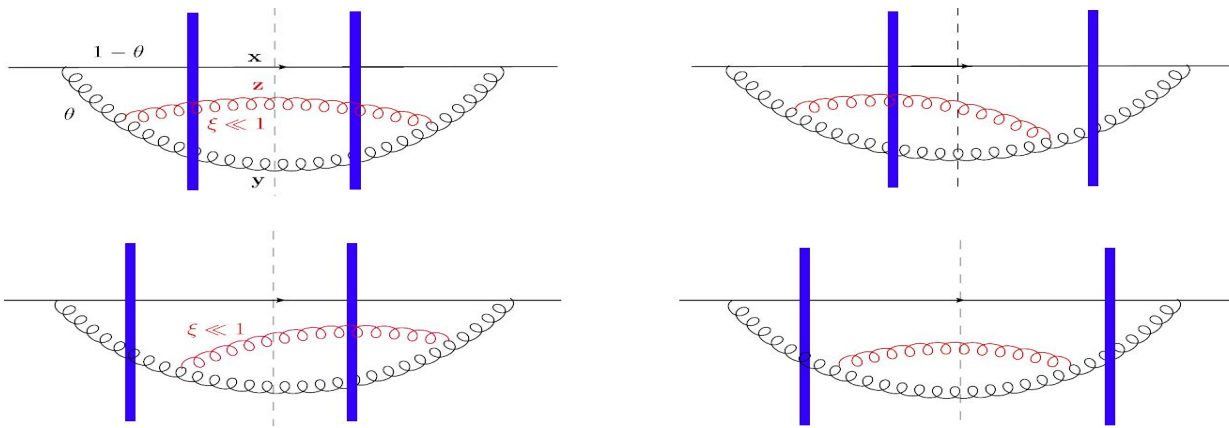


The above 4 diagrams precisely reproduce the the BK evolution of the last piece, the dipole $\mathcal{S}(w, \bar{w})$ from the LO dijet cross-section.

$$\frac{d\sigma_{\text{NLO},1}^{qA \rightarrow qg+X}}{dk_1^+ d^2\mathbf{k}_1 dk_3^+ d^2\mathbf{k}_3} \simeq \frac{\bar{\alpha}_s}{(2\pi)^5} \frac{1 + (1 - \vartheta)^2}{2\vartheta q^+} \delta(q^+ - k_1^+ - k_3^+) \longrightarrow \text{LO result}$$

$$\times \int_{\bar{x}, \bar{z}', x, z'} e^{-ik_1 \cdot (x - \bar{x}) - ik_3 \cdot (z' - \bar{z}')} \frac{(x - z') \cdot (\bar{x} - \bar{z}')}{(x - z')^2 (\bar{x} - \bar{z}')^2}$$

$$\times \frac{\bar{\alpha}_s}{2\pi} \int_0^1 \frac{d\xi}{\xi} \int_z \frac{2(w - z) \cdot (\bar{w} - z)}{(w - z)^2 (\bar{w} - z)^2} [\mathcal{S}(w, \bar{w}) - \mathcal{S}(w, z) \mathcal{S}(z, \bar{w})] \longrightarrow \text{BK evolution of } \mathcal{S}(w, \bar{w})$$



$$\frac{d\sigma_{\text{NLO},2}^{qA \rightarrow qg+X}}{dk_1^+ d^2k_1 dk_3^+ d^2k_3}$$

$$\simeq \frac{\bar{\alpha}_s}{(2\pi)^5} \frac{1 + (1 - \vartheta)^2}{2\vartheta q^+} \delta(q^+ - k_1^+ - k_3^+) \times \int_{\bar{x}, \bar{y}, x, y} e^{-ik_1 \cdot (x - \bar{x}) - ik_3 \cdot (y - \bar{y})} \frac{(x - y) \cdot (\bar{x} - \bar{y})}{(x - y)^2 (\bar{x} - \bar{y})^2}$$

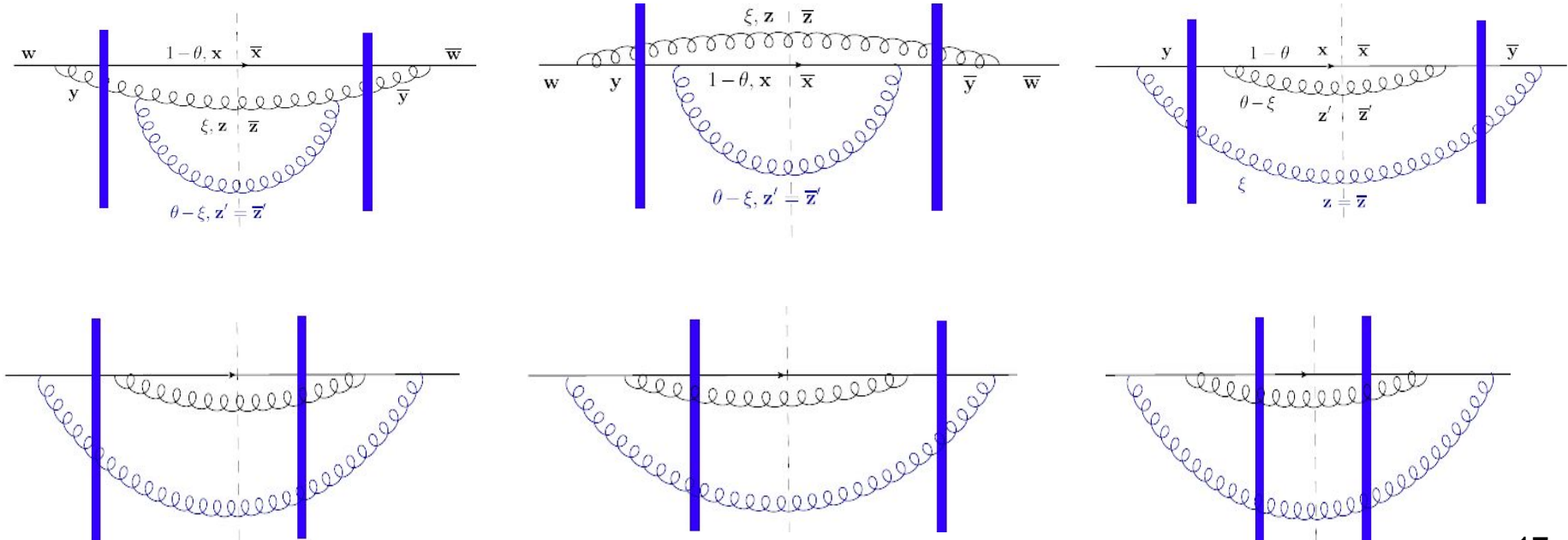
→ LO result

$$\times \frac{\bar{\alpha}_s}{2\pi} \int_0^1 \frac{d\xi}{\xi} \int_z \frac{(y - z) \cdot (\bar{y} - z)}{(y - z)^2 (\bar{y} - z)^2} \times \left\{ \begin{aligned} & \left[\mathcal{S}(x, \bar{x}) \mathcal{S}(y, \bar{y}) - \mathcal{Q}(x, y, z, \bar{x}) \mathcal{S}(\bar{y}, z) \right. \\ & \left. - \mathcal{Q}(x, z, \bar{y}, \bar{x}) \mathcal{S}(z, y) + \mathcal{Q}(x, y, \bar{y}, \bar{x}) \right] \mathcal{S}(y, \bar{y}) \\ & \left. + 2 \left[\mathcal{S}(y, \bar{y}) - \mathcal{S}(y, z) \mathcal{S}(z, \bar{y}) \right] \mathcal{Q}(x, y, \bar{y}, \bar{x}) \right\}$$

→ BK evolution of $\mathcal{Q}(x, y, \bar{y}, \bar{x}) \mathcal{S}(y, \bar{y})$

Recovering the Real DGLAP Evolution

In the collinear limit, when the separation between partons become arbitrarily large, we recover the DGLAP evolution of the initial / final quark state distribution.



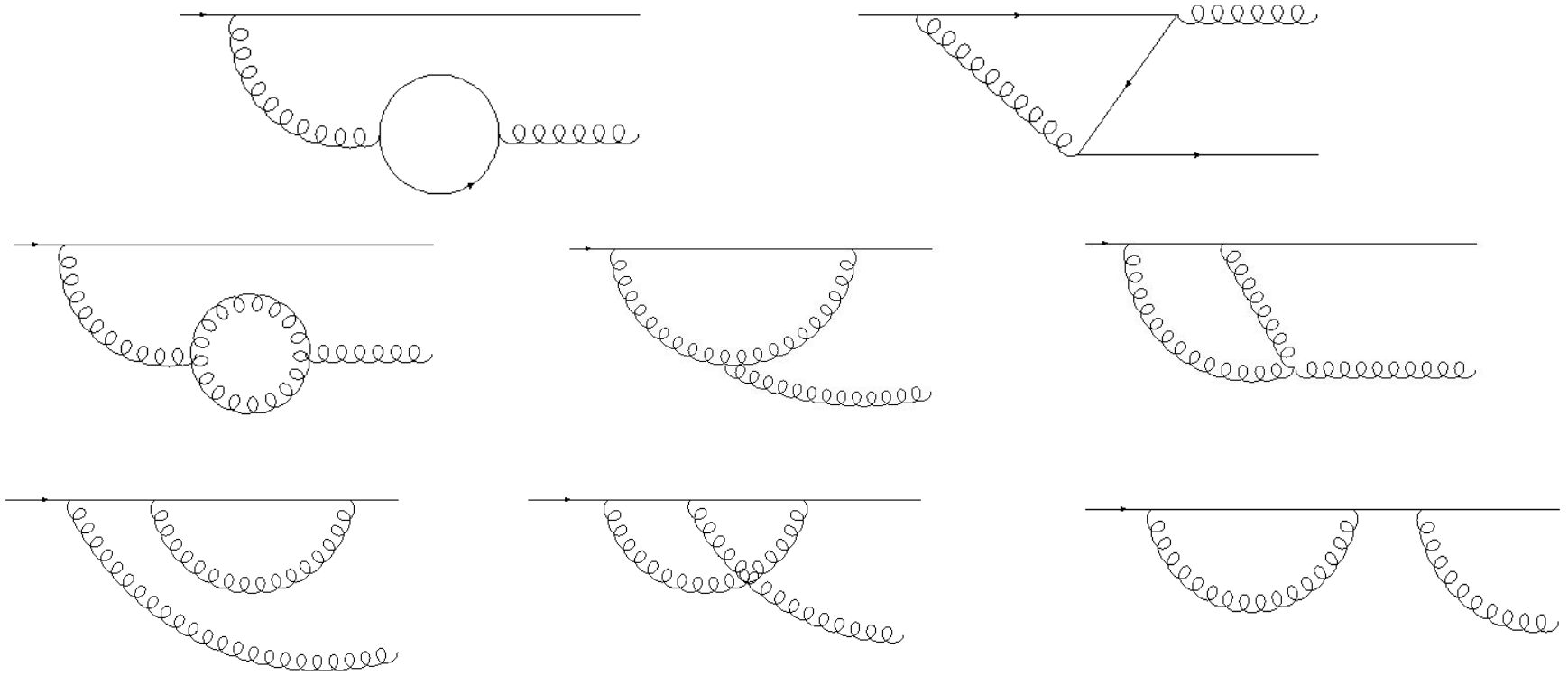
Combining the relevant four contributions:

$$\begin{aligned}
\frac{d\sigma_{(1)\text{rNLO},1}^{qA\rightarrow qg+X}}{dp^+ d^2\mathbf{p} dk^+ d^2\mathbf{k}} &\simeq \frac{4\alpha_s C_F}{(2\pi)^6 (q^+)^2 (1-\xi)} P_{q\rightarrow g}\left(\frac{x_2}{x_1+x_2}\right) \\
&\times \int_{\bar{x}, \bar{z}', x, z'} e^{-i\mathbf{p}\cdot(x-\bar{x})-i\mathbf{k}\cdot(z'-\bar{z}')} \frac{(\mathbf{x}-z')\cdot(\bar{x}-\bar{z}')}{(\mathbf{x}-z')^2(\bar{x}-\bar{z}')^2} \\
&\times \left[Q(x, z', \bar{z}', \bar{x}) \mathcal{S}(z', \bar{z}') - \mathcal{S}(x, z') \mathcal{S}(z', \bar{y}) - \mathcal{S}(y, \bar{z}') \mathcal{S}(\bar{z}', \bar{x}) + \mathcal{S}(y, \bar{y}) \right] \\
&\times \frac{4\alpha_s C_F}{(2\pi)^2} P_{q\rightarrow g}(\xi) \int_z \frac{(\mathbf{y}-z)\cdot(\bar{\mathbf{y}}-z)}{(\mathbf{y}-z)^2(\bar{\mathbf{y}}-z)^2}.
\end{aligned}$$

The result above is precisely the result of one “real” step in the DGLAP evolution of the quark distribution inside the proton:

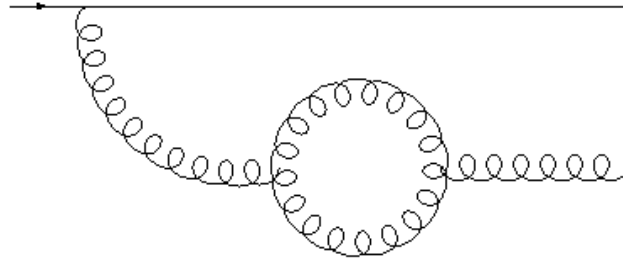
$$x\Delta q_f(x, \mu^2) \equiv \frac{\alpha_s C_F}{\pi} \int_0^{1-x} d\xi \frac{x}{1-\xi} q_f\left(\frac{x}{1-\xi}, \mu^2\right) P_{q\rightarrow g}(\xi) \ln \frac{\mu^2}{\Lambda^2}$$

The Virtual Contributions



The Generic Structure

L diagrams contain both UV and soft divergences.



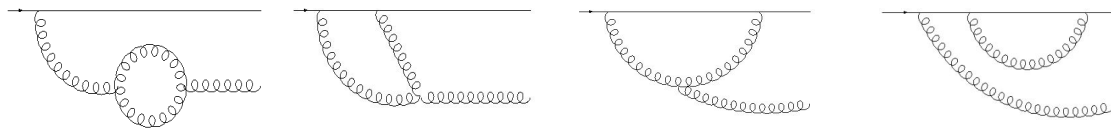
The gluon loop after using dimreg and sharp cutoff regularizations:

$$|\psi_\lambda^\alpha\rangle_{qq}^2 = \int_0^1 d\vartheta \int d^2\tilde{\mathbf{k}} \frac{g^3 N_c t_{\beta\alpha}^a \phi_{\lambda_1\lambda}^{ij}(\vartheta) \tilde{\mathbf{k}}^j \sqrt{q^+}}{4(2\pi)^5 \sqrt{2\vartheta} \tilde{\mathbf{k}}^2} \left(\left[\frac{11}{3} + 4 \ln \left(\frac{\Lambda}{\vartheta q^+} \right) \right] \left[-\frac{2}{\epsilon} + \ln \left(\frac{\tilde{\mathbf{k}}^2}{\mu_{MS}^2} \right) \right] \right. \\ \left. + 2 \ln^2 \left(\frac{\Lambda}{\vartheta(1-\vartheta)q^+} \right) - \frac{67}{9} + \frac{2\pi^2}{3} - \frac{11}{3} \ln(1-\vartheta) - 2 \ln^2(1-\vartheta) \right) \left| q_{\lambda_1}^\beta((1-\vartheta)q^+, (1-\vartheta)\mathbf{q} - \tilde{\mathbf{k}}) g_i^a(\vartheta q^+, \vartheta\mathbf{q} + \tilde{\mathbf{k}}) \right\rangle$$

Two types of IR logs are involved: $\ln \left(\frac{\Lambda}{q^+} \right) \ln \left(\frac{\tilde{\mathbf{k}}^2}{\mu_{MS}^2} \right)$ and $\ln^2 \left(\frac{\Lambda}{\vartheta(1-\vartheta)q^+} \right)$

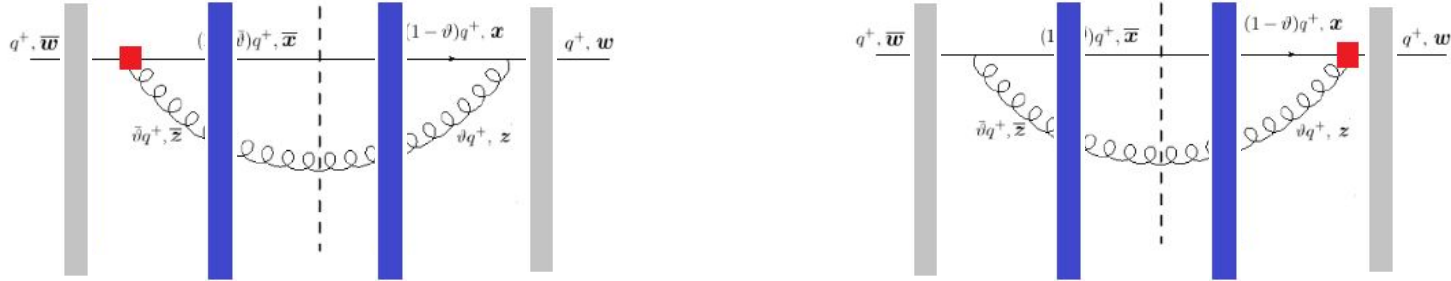
Cancellation of the Soft IR logs

The IR logs cancellation pattern is:



	$ \psi_\lambda^\alpha\rangle_{qg}^2$	$ \psi_\lambda^\alpha\rangle_{qg}^3$	$ \psi_\lambda^\alpha\rangle_{qg}^4$	$ \psi_\lambda^\alpha\rangle_{qg}^5$
$\ln\left(\frac{\Lambda}{q^+}\right) \ln\left(\frac{\tilde{\mathbf{k}}^2}{\mu_{MS}^2}\right)$	4	-3	1	-2
$\ln^2\left(\frac{\Lambda}{\vartheta(1-\vartheta)q^+}\right)$	2	-2	1	-1

The Contribution for the Cross Section



Resulting with the following contribution to the beta function / cusp anomalous dimension:

$$\begin{aligned} \frac{d\sigma_{\text{LO}}^{qA \rightarrow qg+X}}{dp^+ d^2\mathbf{p} dk^+ d^2\mathbf{k}} &= \frac{2\alpha_s^2 C_F [1 + (1 - \vartheta)^2]}{(2\pi)^6 \vartheta q^+} \delta(q^+ - k^+ - p^+) \\ &\times \int_{\mathbf{x}, \bar{\mathbf{x}}, \mathbf{z}, \bar{\mathbf{z}}} \frac{\mathbf{X} \cdot \bar{\mathbf{X}}}{\mathbf{X}^2 \bar{\mathbf{X}}^2} e^{-i\mathbf{p} \cdot (\mathbf{x} - \bar{\mathbf{x}}) - i\mathbf{k} \cdot (\mathbf{z} - \bar{\mathbf{z}})} K(\mathbf{X}, \bar{\mathbf{X}}, \vartheta) \\ &\times [S_{qg\bar{q}g}(\mathbf{x}, \mathbf{z}, \bar{\mathbf{x}}, \bar{\mathbf{z}}) - S_{qg\bar{q}}(\mathbf{x}, \mathbf{z}, \bar{\mathbf{w}})] - S_{q\bar{q}g}(\mathbf{w}, \bar{\mathbf{x}}, \bar{\mathbf{z}}) + \mathcal{S}(\mathbf{w}, \bar{\mathbf{w}})] \end{aligned}$$

$$K(\vartheta, \mathbf{X}, \bar{\mathbf{X}}) = \beta \ln(\mathbf{X}^2 \bar{\mathbf{X}}^2 \hat{\mu}_{\overline{MS}}^4) + \gamma(\vartheta) + \mathcal{I}(\vartheta) + F(\vartheta)$$

$$\beta \equiv \frac{11}{3} N_c - \frac{2}{3} N_f$$

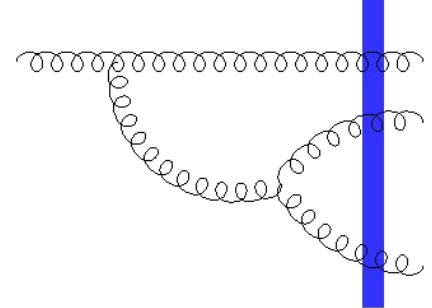
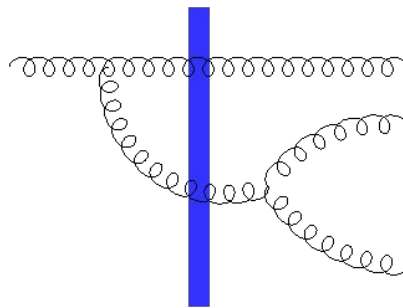
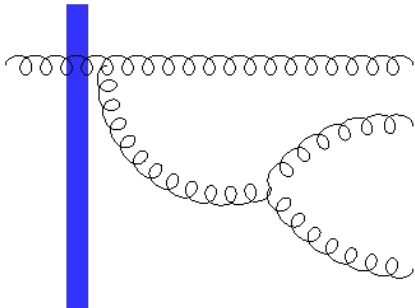
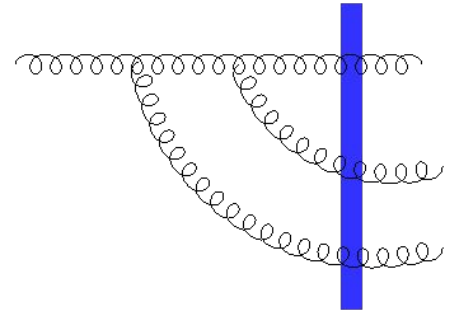
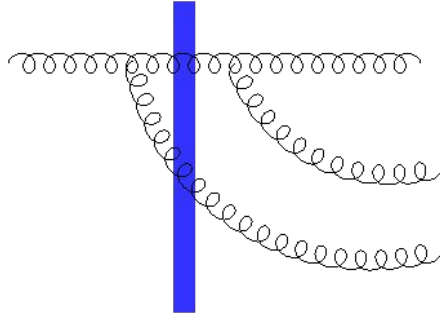
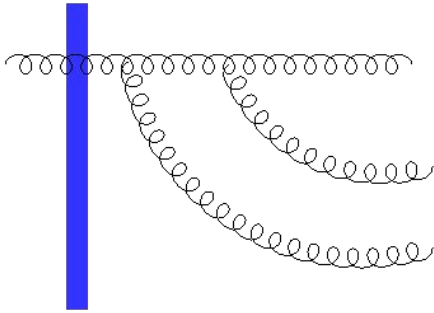
$$\Delta_\gamma(\vartheta) \equiv \left[\frac{2}{3} N_f + \left(3Li_2(\vartheta) + \frac{1}{2} \ln \left(e^{\frac{13}{3}} \vartheta^2 (1 - \vartheta) \right) \right) N_c \right] \ln(1 - \vartheta)$$

$$\gamma(\vartheta) \equiv \left(\frac{67}{9} - \frac{\pi^2}{3} \right) N_c - \frac{10}{9} N_f + \Delta_\gamma(\vartheta)$$

$$\mathcal{I}(\vartheta) \equiv \left(3 + 4 \ln \left(\frac{\Lambda}{\vartheta q^+} \right) \right) N_c \int \frac{d^2\tilde{\mathbf{p}}}{\tilde{\mathbf{p}}^2}$$

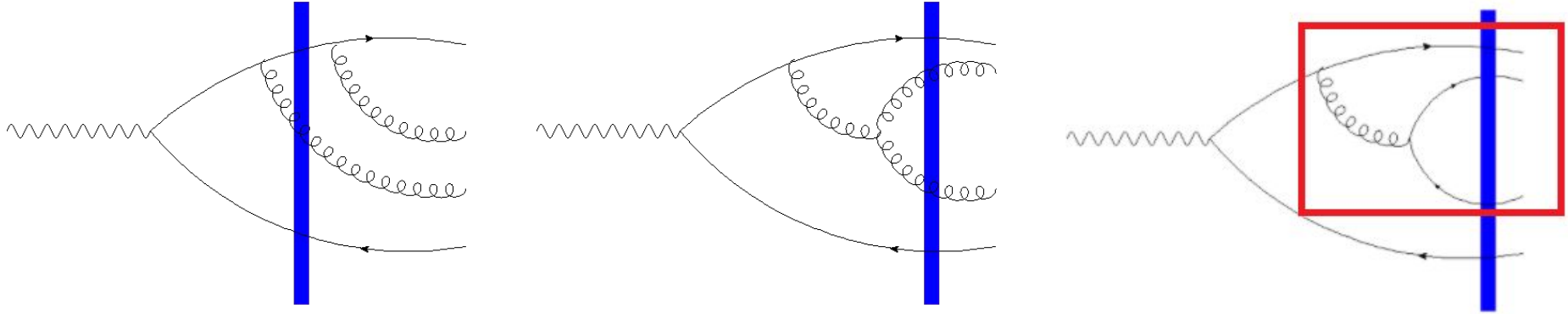
What's Next?

Including the gluon channel: the contributions which involve incoming gluon are necessary in order to fully absorb all the various divergences in a consistent manner (also improved accuracy outside low-x regime).

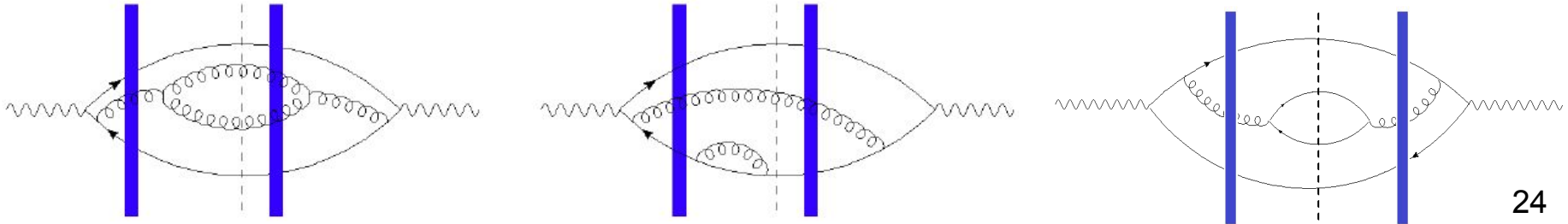


From pA to eA

Most of the computation of the NNLO outgoing photon state overlaps the computation of the outgoing quark state



Successful completion will lead to the result NNLO DIS structure functions and various interesting inclusive / exclusive cross sections.



Summary

- 1) We computed the full (real and virtual) NLO outgoing state and dijet production cross section of an incoming quark.
- 2) Short-distance poles has been shown to cancel between pairs of diagrams.
- 3) Full match has been established between the eikonal limit of the result and the action of the real part of JIMWLK acting on the LO cross section for forward dijet production.
- 4) Full match has been established with DGLAP evolution in the collinear limit.
- 5) The L diagrams have been shown to reproduce the beta function and cusp anomalous dimension. The IR logs cancel after combining all the L diagrams.